GEORGE BROWN PRESS
JOURNALS, BOOKS & PROCEEDINGS

Journal of Medicine and Life Sciences

Article

Modeling Degenerative Disc Disease under a Stochastic Disease Random Branching Process

Wenyue Xia [1,*]

[1] Huawei HiSilicon Semiconductor Co., Ltd., Shenzhen, Guangdong, China
* Correspondence: Wenyue Xia, Huawei HiSilicon Semiconductor Co., Ltd., Shenzhen, Guangdong, China

Abstract: Degenerative disc disease (DDD) is a leading source of neck and lower back pain, especially among older adults and individuals in high-load occupations. Clinical practice currently struggles to predict DDD quantitatively, delaying effective intervention. This project proposes a three-stage, continuous stochastic model describing disc degeneration initiation, progression, and propagation to adjacent discs. By incorporating measurable disc indicators — such as height loss, displacement, and annulus tears — into a physics–statistics-based framework, we derive DDD metrics that estimate disc lifespans, the probability of multi-level degeneration, and time-to-pain events. We then interpret these metrics to guide personalized decisions about whether to treat only severely degenerated discs or also discs likely to degenerate soon, factoring in age, occupation, and lifestyle. With real-time MRI data, the model updates dynamically, strengthening its clinical relevance. Our findings could enhance early detection, inform optimal surgical timing, and improve outcomes for at-risk populations, including Hong Kong's aging workforce.

Keywords: degenerative disc disease (DDD); stochastic modeling; disc degeneration; MRI; personalized treatment

1. Introduction

Degenerative disc disease (DDD) represents a significant health concern due to its link with chronic neck and lower back pain (LBP). It arises from gradual deterioration within the intervertebral discs — structures in the spine that cushion vertebrae and absorb mechanical loads. Although the term "disease" is used, DDD can be considered part of the natural aging process, in which discs lose water content, and microstructural changes occur. Yet, this phenomenon is not limited solely to aging populations: individuals who frequently perform activities placing high loads on the spine — such as stevedores, commercial drivers, and certain trading or industrial workers — also face elevated risk. In a densely populated region like Hong Kong, which is home to a large community of senior citizens along with occupationally vulnerable groups (for example, taxi drivers and laborers), DDD is poised to become an even more prevalent source of disability and diminished quality of life. Despite the strong social and healthcare implications of DDD, current clinical management often struggles with a lack of quantitative tools for early detection, prediction, and personalized intervention.

Many DDD patients only become aware of the condition once disc degeneration has progressed enough to elicit persistent pain. Typically, an individual experiences discomfort or sharp pain, prompting a clinical visit — possibly leading to diagnostic imaging via Magnetic Resonance Imaging (MRI). This scan may reveal reduced disc height, tears in the annulus fibrosus (AF), or visible degenerative changes such as disc bulging or displacement. Yet doctors have limited capacity to forecast how or when adjacent discs might start or accelerate their own degeneration. While the MRI findings offer a snapshot of the

Received: 10 February 2025
Revised: 13 February 2025
Accepted: 18 February 2025
Published: 20 February 2025

Copyright: © 2025 by the authors. Submitted for possible open access publication under the terms and conditions of the Creative Commons Attribution (CC BY) license (https://creativecommons.org/licenses/by/4.0/).

current state, they do not readily deliver a dynamic timeline: the subsequent progression of each disc remains unclear.

In this context, a quantitative characterization of DDD could bring significant benefits. By rigorously modeling each disc's behavior — spanning how long it takes for degeneration to begin, how rapidly it worsens, and how it may propagate to adjacent levels — clinicians could receive predictive insights. They would be better able to advise a patient that "Disc L4-L5 is likely to develop serious pathology in the coming year," or "Disc C5-C6 is at moderate risk, but surgical intervention is not necessary yet." Such data-driven predictions might also open the door to more personalized prevention programs (for instance, physical therapy regimens targeted at fortifying certain spinal segments) or early interventions (like removing or replacing a disc before the onset of severe pain).

However, establishing these predictive models is far from trivial. First, the degenerative processes in intervertebral discs are complex, involving changes in disc hydration, microcracks or tears in the annulus fibrosus, and chemical and biomechanical shifts that can accelerate or decelerate over time. Second, discs do not degenerate in isolation. The mechanical environment of the spine means that once one level is compromised, the load distributions on adjacent segments can change, creating either compensatory mechanisms or new stress concentrations that hasten the degeneration of neighboring discs. Third, external factors — aging, repeated heavy lifting, prolonged sitting (as for taxi drivers), or awkward postures — create a dynamic interplay that modifies the rate and severity of disc degeneration. To address the pressing knowledge gap, one must capture both the time-dependent and spatial elements of disc behavior.

In this paper, we aim to develop a rigorous, physics-statistics-based modeling framework that interprets disc degeneration as a three-stage continuous stochastic process: (1) initiation, (2) increment (i.e., progression), and (3) propagation (i.e., transferring degenerative load or impetus to adjacent discs). We propose to analyze disc height loss, displacement, annulus fibrosus tears, and other morphological indicators collectively, combining them into a single measure of "disc degeneration level." By mapping these levels into a stochastic model, we intend to derive mathematical distributions for disc lifespans, or "time to serious damage." Our approach's novelty stems from embedding multi-directional branching within the model, capturing how a disc under stress not only deteriorates but may also exert a degenerative influence on contiguous discs in multiple directions.

Once the fundamental course of DDD is described quantitatively, we will define "DDD metrics" — such as "the probability that a certain disc has reached a threshold of degenerative severity at time t," or "the expected number of degenerated discs by age 65." We will link those metrics to clinically meaningful outcomes, including the onset of pain. Although not all degenerative changes trigger pain, a subset of disc conditions (e.g., disc herniation impinging on a nerve root) are known to cause discomfort or radiculopathy. We plan to incorporate a bridging mechanism, so that once a disc's degeneration surpasses some threshold, the hazard rate of pain events in that disc drastically increases. This allows us to estimate the distribution of "time to first pain" or the probability that disc L5-S1 is responsible for a patient's symptoms at a given future date.

Overall, tackling degenerative disc disease with a three-stage framework of initiation, increment, and propagation, and linking the mathematical outcomes to the real question of "when does the patient feel pain?" can lead to a more robust, evidence-driven strategy for both prevention and treatment. By bridging the gap between purely imaging-based diagnosis and long-term predictive analytics, we aspire to guide clinicians, patients, and healthcare policymakers toward interventions at the right time in the right population — particularly in regions like Hong Kong, where the prevalence of DDD continues to rise due to demographic and occupational factors.

2. Literature Review

Most of current studies on DDD emphasize on the impact of loading on the change of discs' morphological and mechanical properties. The level of static compressive loading, together with the magnitude and number of cycles of dynamic compression loading, is crucial to the change of disc's morphological indicators, elastic modulus, fatigue strength and stiffness parameter. Notably, impact compression/bending loading induces much severer morphological and mechanical damage than static loading [1]. Discs' survival rate and time-to-AF-displacement under cyclic compression and shear loading are experimentally observed in [2]; the results indicate that shear loading is the primary reason of discs' displacement. Discs' degeneration level also affects its morphological and mechanical properties. Compared with intact discs, degenerated discs' morphological properties [3] and mechanical properties [4] are more sensitive to different types of loading such as flexion, extension, bending, shearing and torsion. Specifically, disc's stiffness decreases while stability increases w.r.t. the degeneration level; morphologically, disc's RoM increases and then decreases w.r.t the degeneration level. Studies also identify that discs' degeneration interact with each other, where the interaction is particularly apparent for degenerated discs. The dependency among discs is morphologically observed in MRI, based on which statistical analysis is conducted to obtain the distribution of the degenerated discs over the entire spine. The intradiscal pressure and stiffness of a degenerated disc's superior and inferior segments increase as compensation for the loss of RoM in the degenerated disc. The position of the degenerated disc also affects the RoM of its adjacent discs/segments [5].

Human disc degeneration modeling can be also studied from the perspective of reliability modeling, assessment, and optimization of a population of components [6]. Building on the results, effective reliability testing [7], monitoring methodologies [8], control strategy [9], criticality analysis [10-12], and inspection and maintenance policy [13-17]. However, these studies fail to take the complex stochastic dependency among the components into consideration, and therefore, these methodologies are inapplicable to modeling the DDD problem.

3. Discs' Degeneration Initiation, Increment and Propagation Modeling

3.1. Discs' Degeneration Process

Human spine contains 23 discs that absorb the shock between vertebrae and control the spine motion in three planes (flexion-extension, axial rotation and lateral bending). For arbitrarily individual disc (say, disc i, i = 1, ...,23),its degeneration is a continuous cumulative damage process *w.r.t.* factors such as age, load induced by daily activities and the degeneration level of its adjacent discs. Defining $D_i(t)$ as the degeneration level of disc *i* at time *t*, we analyze $D_i(t)$ as a three-stage process:

Degeneration initiation stage $t \in \left(0, T_i^{DIT}\right)$: T_i^{DIT} is the time instant when disc *i*'s degeneration initiates (i.e., disc *i*'s time-to-degeneration-initiation); fatigue damage induced by daily activities, shock damage induced by sudden injury and aging effect accumulate to initiate disc's degeneration at time T_i^{DIT} ; disc *i* is non-degenerated during this stage, i.e., $D_i(t) = 0 \text{ for } t \in \left(0, T_i^{DIT}\right)$;

Degeneration increment stage $t \in \left(T_i^{DIT}, T_i^{DPT}\right)$: disc *i*'s degeneration initiates at T_i^{DIT} and reaches its "degeneration propagation threshold" (DPT) D_i^{DPT} at time instant T_i^{DPT} , i.e., $D_i\left(T_i^{DPT}\right) = D_i^{DPT}$;

Degeneration propagation stage $t \in \left(T_i^{DPT}, T_i^{PT}\right)$: disc *i*'s degeneration level reaches D_i^{DPT} at time T_i^{DPT} and the degeneration is propagated to adjacent discs (*i* - 1) and (*i* + 1) to accelerate their degeneration processes; meanwhile, disc *i*'s degeneration continues to increase.

Such a pattern applies to all discs, where the degeneration initiates and increases within individual disc and propagates among discs. Note that for arbitrary disc, its degeneration process dynamically interacts with that of its adjacent discs. Specifically, disc *i*'s degeneration accelerates twice as discs (*i* - 1) and (*i* + 1) reach their DPTs at time instants T_{i-1}^{DPT} and T_{i+1}^{DPT}, propagating the degeneration to disc *i*. Notably, i) D_i^{DIT} and D_i^{DPT} $\forall$i = 1, ...,23, are stochastically given and vary from individual to individual and ii) all discs' degeneration processes are stochastic *w.r.t.* time due to the random variation of human daily activities, i.e., T_i^{DIT} and T_i^{DPT} are random variables with $T_i^{DIT} < T_i^{DPT}$ $\forall$i = 1, ...,23.

3.2. Degeneration Process Modeling

To understand the degeneration process of all discs, we will need to model the degeneration initiation and increment of individual disc as well as the degeneration propagation among multiple discs.

3.2.1. Degeneration initiation of disc i

The key to model the degeneration initiation of disc *i* is to identify the distribution of the time when disc *i*'s degeneration initiates (i.e., T_i^{DIT}). Disc *i*'s position p_i, patient's age a, loading during the degeneration initiation stage ($\int_0^{T_i^{DIT}} \underset{\sim}{Z}_i(t)dt$), degeneration status of adjacent discs (in terms of T_{i-1}^{DPT} and T_{i+1}^{DPT}), potential sudden injury q_i, the degeneration process randomness (ε) and other degeneration-related parameters (Ψ_T) jointly determine T_i^{DIT} (Eq. (1)). We will then derive the physics-statistics-based explicit form of $F_T(\cdot)$; specifically, we will either model the damage accumulation process as an IG (or Gamma) process with its parameters being functions of the above mentioned factors, or model disc's degeneration rate as a nonparametric function (e.g., proportional hazard (PH) model and proportional odds (PO) model) *w.r.t.* the above factors.

$$T_i^{DIT} = F_T\left(T_{i-1}^{DPT}, T_{i+1}^{DPT}, q_i, p_i, a, s, w, g, \int_0^{T_i^{DIT}} \underset{\sim}{Z}_i(t)dt, \varepsilon_T; \Psi_T\right) \tag{1}$$

3.2.2. Degeneration increment of disc i

The key to model the degeneration increment process of disc *I* is to explore the distribution of $D_i(t)$. Note that $D_i(t)$ is dependent on disc's degeneration initiation process, i.e., $D_i(t) = \int_0^t D_i\left(t \middle| T_i^{DIT}\right) dT_i^{DIT}$. As previously discussed, the degeneration process of disc *i* accelerates twice when the degeneration propagates from its adjacent discs (*i* - 1) and (*i* +1). To reflect this, we define $D_{i\_s}\left(t \middle| T_i^{DIT}\right)$ as disc *i*'s degeneration increment "amount" after *s* times ($s = 0,1,2$) of accelerations and write $D_i\left(t \middle| T_i^{DIT}\right)$ *w.r.t.* T_{i-1}^{DPT} and T_{i+1}^{DPT} (Eq. (2)).

$$D_i\left(t \middle| T_i^{DIT}\right) = \begin{cases} D_{i\_2}\left(\max\left(0, t - T_i^{DIT}\right)\right) & \text{if } A \le T_i^{DIT} \\ D_{i\_1}\left(\min\left(A - T_i^{DIT}, t - T_i^{DIT}\right)\right) + D_{i\_2}\left(\max\left(0, t - A\right)\right) & \text{if } B \le T_i^{DIT} \le A \\ D_{i\_0}\left(\min\left(B - T_i^{DIT}, t - T_i^{DIT}\right)\right) + D_{i\_1}\left(\min\left(A - B, t - B\right)\right) + D_{i\_2}\left(\max\left(0, t - A\right)\right) & \text{if } T_i^{DIT} \le B \end{cases} \tag{2}$$

where $A = \max\left\{T_{i-1}^{DPT}, T_{i+1}^{DPT}\right\}$, $B = \min\left\{T_{i-1}^{DPT}, T_{i+1}^{DPT}\right\}$ and $D_{i\_s}(0) = 0$.

Including all factors that impact $D_i\left(t \middle| T_i^{DIT}\right)$ and referring to Eq. (2), we model $D_i(t)$ in Eq. (3). We will derive the explicit form of Eq. (3) by referring to the similar procedures when deriving Eq. (1).

$$D_i(t) = \int_{T_i^{DIT}=0}^{t} \sum_{\forall s} F_D\left(\max\left(0, t - T_i^{DIT}\right); T_{i-1}^{DPT}, T_{i+1}^{DPT}, q_i, p_i, a, w, g, s, \int_{T_i^{DIT}}^{t} \underset{\sim}{Z}_i(\mu)d\mu, \int_{T_i^{DIT}}^{t} D_i(\mu)d\mu, \varepsilon_D, \Psi_D\right) dT_i^{DIT} \tag{3}$$

Based on Eq. (3), we will obtain the distributions of $T_i^{DPT}, i=1,...,23$ (Eq. (4)). Note that terms T_i^{DIT}, T_{i-1}^{DPT} and T_{i+1}^{DPT} in Eqs. (1) - (3) dynamically interact; this requires us to explore the joint distribution of $T_i^{DPT}, i=1,...,23$ and that of $T_i^{PT}, i=1,...,23$.

$$P\left(T_i^{DPT}>t\right)=P\left(D_i(t)<D_i^{DPT}\right) \tag{4}$$

3.2.3. Degeneration Propagation among Discs

In addition to modeling the degeneration initiation and increment of individual disc, we also need to capture the two-direction degeneration propagation process. We will develop a convolution model and use combinatorial approach to assess the time and "sequence" in which discs' propagations occur. The two models will enable us to investigate the degeneration process of all discs in terms of the sum of specific (or, all) discs' degeneration level (i.e., $\sum_{\forall \underset{\sim}{i}} P\left(\sum_{\forall i\in \underset{\sim}{i}} D_i(t)<\bar{D}\right)$) and the distribution of degenerated discs (i.e., $P\left(\underset{\sim}{I}(t)=\underset{\sim}{i}\right)$) at arbitrary time instant t, where $\bar{D}$ is arbitrarily given degeneration level and $\underset{\sim}{I}(t)$ is a random vector of degenerated discs at time t, e.g., $P\left(\underset{\sim}{I}(t)=(2,6,7)\right)$ is the probability that discs 2,6 and 7 are degenerated at time t.

3.3. Discs' Reliability Metrics and DDD-Induced Pain

As is clinically investigated, a DDD-induced pain occurs either when the degeneration level of arbitrary degenerated disc (say, disc i) reaches its "pain threshold" D_i^{PT} at random time instant T_i^{PT} (i.e., $D_i\left(T_i^{PT}\right)=D_i^{PT}$) or when the sum of specific (or, all) discs' degeneration level reaches an "overall pain threshold" D^{OPT} at random time instant T^{OPT} (i.e., $\sum_{\forall i:D_i\left(T^{OPT}\right)>0} D_i\left(T^{OPT}\right)=D^{OPT}$), whichever is earlier. Writing the time when DDD-induced pain occurs as $T^{PT}=\min\left\{T^{OPT},T_i^{PT}, i=1,...,23\right\}$, we will explore the distribution of T^{OPT} and T_i^{PT} (Eqs. (5) and (6)), based on which we will thoroughly investigate the statistical metrics of T^{PT} such as its distribution (Eq. (7)), expectation (Eq. (8)) and the probability that the pain is induced by disc i (Eq. (9)). We further define $R_{PT}(t)=\text{Prob}\left(T^{PT}>t\right)$ as "*discs' reliability*" at time t and $E\left(T^{PT}\right)$ as "*discs' DDD lifetime*".

$$P\left(T_i^{PT}>t\right)=P\left(D_i\left(t\middle|T_i^{DIT}\right)<D_i^{PT}\right) \tag{5}$$

$$\text{Prob}\left(T^{OPT}>t\right)=\sum_{\forall \underset{\sim}{i}} P\left(T^{OPT}>t \text{ and } I(t)=\underset{\sim}{i}\right)=\sum_{\forall \underset{\sim}{i}} P\left(\sum_{\forall i\in \underset{\sim}{i}} D_i(t)<D^{OPT} \text{and } D_i(t)>0\ \forall i\in \underset{\sim}{i}\right) \tag{6}$$

$$\text{Prob}\left(T^{PT}>t\right)=\text{Prob}\left(D_i(t)<D_i^{PT}\forall\left\{i:D_i(t)\ >0\right\} \text{ and } \sum_{\forall i:D_i(t)>0} D_i(t)<D^{OPT}\right) \tag{7}$$

$$E\left(T^{PT}\right)=\int_0^{\infty}\text{Prob}\left(T^{PT}>t\right)dt\ \text{Prob}\left(T_i^{PT}=T^{PT}\right) \tag{8}$$

Note that the models proposed above also apply for discs' reliability metrics prediction when specific (or, all) discs' degeneration status are known. such as obtained in MRI. To illustrate, knowing that discs $\underset{\sim}{i}'$ (where $\underset{\sim}{i}$ is the vector of all degenerated discs) are degenerated at time t' with $D_{i'}(t')=D_{i'\_t'},\forall i'\in \underset{\sim}{i}'$, we predict the mean residual life (*MRL*) to DDD-induced pain ($MRL\left(T^{PT}\middle|D_{i'}(t')=D_{i'\_t'},\forall i'\in \underset{\sim}{i}'\right)$) in Eq. (9).

$$\begin{aligned} &MRL\left(T^{PT}\middle|D_{i'}(t')=D_{i'\_t'},\forall i'\in \underset{\sim}{i}'\right)\\ &=\int_{t'}^{\infty} P\left(\sum_{i\in \underset{\sim}{i}} D_i(\eta)<D^{OPT} \text{ and } D_i(\eta)<D_i^{PT}\ \forall i\in \underset{\sim}{i}\ \middle|D_{i'}(t')=D_{i'\_t'},\forall i'\in \underset{\sim}{i}'\right)d\eta\\ &=\int_{t'}^{\infty}\sum_{\forall \underset{\sim}{i}}\sum_{\forall \underset{\sim}{i}'} P\left(\sum_{\forall i\in \underset{\sim}{i}} D_i(\eta-t')<\left(D^{OPT}-\sum_{i'\in \underset{\sim}{i}'} D_{i'\_t'}\right) \text{ and } D_i(\eta-t')<D_i^{PT}-D_{i\_t}\forall i\in \underset{\sim}{i}\right)d\eta \end{aligned} \tag{9}$$

4. Case Study

We consider a segment of two discs, shown in Figure 1, whose individual degradation processes follow a Wiener process with drift parameter μ_i and diffusion parameter σ_i^2; when the disc i reaches a specified threshold D_i, the degradation propagates among the discs and their degradation rates accelerate to $\tilde{\mu}_i, i = 1,2$. The associated parameters are given in Table 1. Length is measured in millimeters (mm), and time is measured in years.

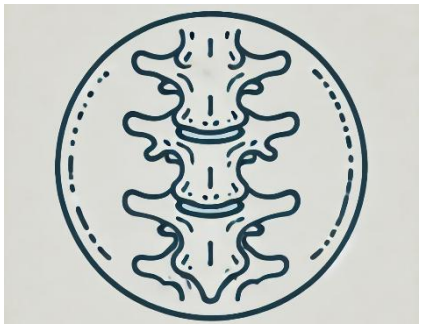

Figure 1. A schematic of a segment of two discs.

Table 1. The parameters associated with the discs' degradation processes.

μ_1	σ_1^2	μ_2	σ_2^2	D_1	D_2	μ_1%	μ_2%
0.2	0.015	0.25	0.02	0.6	0.6	0.3	0.4

Based on the model proposed in this study, we provide an estimation of the time required for a transition from healthy discs to those necessitating surgical intervention, under different clinical intervention criteria. Specifically:

1) Criterion 1**:** Surgical intervention is considered when the cumulative degradation reaches 2 mm. Under this criterion, the expected time to reach the threshold is approximately 3.6 years, with the 10th percentile estimated at 2.7 years.
2) Criterion 2**:** Surgical intervention is triggered when any one disc experiences a degradation of 1 mm. Under this condition, the expected time is about 2.9 years, with the 10th percentile at 2.6 years.

These results not only provide a clear timeline for intervention under different degradation thresholds but also underscore the sensitivity of the system to the chosen criteria. Our methodology demonstrates robust performance in capturing the interdependency of degradation processes between discs, which is crucial for accurate lifetime analysis.

Furthermore, the analysis indicates that even slight variations in the clinical criteria can lead to significant differences in the predicted time to intervention. This finding emphasizes the importance of carefully selecting degradation thresholds to optimize patient outcomes. Additionally, our sensitivity analysis suggests that the dependency between discs plays a critical role in the progression of degradation, highlighting the potential for personalized management strategies in clinical practice.

Overall, these insights confirm that the proposed modeling framework can effectively quantify degradation dynamics and support the development of more precise, patient-specific intervention protocols.

5. Conclusion

In summary, we have introduced a novel quantitative framework for investigating degenerative disc disease (DDD) as a three-stage continuous stochastic process, capturing disc initiation, progression, and propagation. By merging physics- and statistics-based models with branching mechanisms, we gain a dynamic perspective on how a given disc's degeneration can influence adjacent discs over time. The proposed DDD metrics provide

clinically meaningful insights — ranging from the distribution of disc-specific time-to-degeneration to the probability of multi-level involvement and pain onset. Moreover, by considering MRI snapshots as Bayesian-like evidence, the model can adapt to real patient conditions and update subsequent risk estimations accordingly, thereby facilitating more personalized interventions.

Moving forward, several directions warrant exploration. First, expanding the dataset to include diverse populations — those with varied lifestyles, body mass indices, and comorbidities — would validate the model's robustness across different demographic profiles. Second, integrating advanced imaging parameters (e.g., disc biochemical markers) may refine our understanding of disc microenvironment changes. Third, automated machine-learning approaches could further optimize parameter fitting, enabling real-time forecasting in clinical settings. Finally, randomized trials comparing different surgical or rehabilitative strategies based on model predictions could substantiate the practical benefits of adopting an individualized, data-driven paradigm for DDD management. By pursuing these directions, we anticipate this framework will significantly improve early detection, preventive care, and outcome optimization for patients at risk of degenerative disc disease.

References

1. D. Jamison, M. Cannella, E. C. Pierce, and M. S. Marcolongo, "A comparison of the human lumbar intervertebral disc mechanical response to normal and impact loading conditions," J. Biomech. Eng., vol. 135, no. 9, p. 091009, 2013, doi: 10.1115/1.4024828.
2. S. Gallagher, W. S. Marras, A. S. Litsky, D. Burr, J. Landoll, and V. Matkovic, "A comparison of fatigue failure responses of old versus middle-aged lumbar motion segments in simulated flexed lifting," *Spine*, vol. 32, no. 17, pp. 1832–1839, 2007, doi: 10.1097/01.brs.0000259812.75138.c0.
3. A. L. Nachemson, A. B. Schultz, and M. H. Berkson, "Mechanical properties of human lumbar spine motion segments. Influence of age, sex, disc level, and degeneration," *Spine*, vol. 4, no. 1, pp. 1–8, 1979, doi: 10.1097/00007632-197901000-00001.
4. P.-P. A. Vergroesen, A. J. van der Veen, B. J. van Royen, I. Kingma, and T. H. Smit, "Intradiscal pressure depends on recent loading and correlates with disc height and compressive stiffness," *Eur. Spine J.*, vol. 23, no. 11, pp. 2359–2368, 2014, doi: 10.1007/s00586-014-3450-4.
5. R. N. Natarajan and G. B. Andersson, "Lumbar disc degeneration is an equally important risk factor as lumbar fusion for causing adjacent segment disc disease," *J. Orthop. Res.*, vol. 35, no. 1, pp. 123–130, 2017, doi: 10.1002/jor.23283.
6. Y. Wei, Y. Cheng, and H. T. Liao, "Fleet service reliability analysis of self-service systems subject to failure-induced demand switching and a two-dimensional inspection and maintenance policy," *IEEE Trans. Autom. Sci. Eng.*, Dec. 2024, doi: 10.1109/TASE.2024.3516049.
7. Y. Cheng and E. A. Elsayed, "Design of optimal sequential hybrid testing plans," *IISE Trans.*, vol. 53, no. 7, pp. 830–841, Apr. 2021, doi: 10.1080/24725854.2020.1805828.
8. R. X. Li, J. G. Wu, Y. X. Li, and Y. Cheng, "PeriodNet: Noise-robust fault diagnosis method under varying speed conditions," *IEEE Trans. Neural Netw. Learn. Syst.*, vol. 35, no. 10, pp. 14045–14059, Oct. 2024, doi: 10.1109/TNNLS.2023.3274290.
9. Gao, J. W. Wang, S. Gao, and Y. Cheng, "An integrated robust design and robust control strategy using the genetic algorithm," *IEEE Trans. Ind. Inform.*, vol. 17, no. 12, pp. 8378–8386, Dec. 2021, doi: 10.1109/TII.2021.3056417.
10. C. Y. Zou, J. W. Wang, and Y. Cheng, "The impact of the variability of patient flow and service time on the efficiency of large-scale outpatient systems," *IEEE Trans. Comput. Soc. Syst.*, vol. 10, no. 3, pp. 1230–1240, Jun. 2023, doi: 10.1109/TCSS.2021.3137930.
11. J. W. Wang, Y. Gao, and Y. Cheng, "On time-dependent critical platforms and tracks in metro systems," *Transp. Sci.*, vol. 56, no. 4, pp. 953–971, Jul.–Aug. 2022, doi: 10.1287/trsc.2022.1124.
12. C. Y. Zou, J. W. Wang, and Y. Cheng, "Critical department analysis for large-scale outpatient systems," *IEEE Trans. Comput. Soc. Syst.*, vol. 10, no. 6, pp. 3194–3203, Dec. 2023, doi**:** 10.1109/TCSS.2022.3212121.
13. Y. Cheng, H. T. Liao, and Z. Y. Huang, "Optimal degradation-based hybrid double-stage acceptance sampling plan for a heterogeneous product," *Rel. Eng. Syst. Saf.*, vol. 210, Jun. 2021, Art no. 107544, doi: 10.1016/j.ress.2021.107544.
14. Y. Wei, Y. Cheng, and H. T. Liao, "Optimal resilience-based restoration of a system subject to recurrent dependent hazards," *Rel. Eng. Syst. Saf.*, vol. 247, Jul. 2024, Art no. 110137, doi: 10.1016/j.ress.2024.110137.
15. S. Zhao, Y. Wei, Y. Cheng, and Y. Li, "A state-specific joint size, maintenance, and inventory policy for a k-out-of-n load-sharing system subject to self-announcing failures," *Rel. Eng. Syst. Saf.*, p. 110855, 2025, doi: 10.1016/j.ress.2025.110855.
16. Y. Wei, A. Li, Y. Cheng, and Y. Li, "An optimal multi-level inspection and maintenance policy for a multi-component system with a protection component," *Comput. Ind. Eng.*, p. 110898, 2025, doi: 10.1016/j.cie.2025.110898.

17. Y. Wei and Y. Cheng, "An optimal two-dimensional maintenance policy for self-service systems with multi-task demands and subject to competing sudden and deterioration-induced failures," *Rel. Eng. Syst. Saf.*, vol. 255, p. 110628, 2025, doi: 10.1016/j.ress.2024.110628.

Disclaimer/Publisher's Note: The statements, opinions and data contained in all publications are solely those of the individual author(s) and contributor(s) and not of GBP and/or the editor(s). GBP and/or the editor(s) disclaim responsibility for any injury to people or property resulting from any ideas, methods, instructions or products referred to in the content.